ORIGINAL RESEARCH

Epidermal Growth Factor Receptor Silencing Blunts the Slow Force Response to Myocardial Stretch

María S. Brea, BSc; Romina G. Díaz, PhD; Daiana S. Escudero, BSc; Claudia I. Caldiz, PhD; Enrique L. Portiansky, PhD; Patricio E. Morgan, PhD;* Néstor G. Pérez, PhD;*

***Background*—**Myocardial stretch increases force biphasically: the Frank-Starling mechanism followed by the slow force response (SFR). Based on pharmacological strategies, we proposed that epidermal growth factor (EGF) receptor (EGFR or ErbB1) activation is crucial for SFR development. Pharmacological inhibitors could block ErbB4, a member of the ErbB family present in the adult heart. We aimed to specifically test the role of EGFR activation after stretch, with an interference RNA incorporated into a lentiviral vector (small hairpin RNA [shRNA]-EGFR).

***Methods and Results*—**Silencing capability of p-shEGFR was assessed in EGFR-GFP transiently transfected HEK293T cells. Four weeks after lentivirus injection into the left ventricular wall of Wistar rats, shRNA-EGFR–injected hearts showed ≈60% reduction of EGFR protein expression compared with shRNA-SCR–injected hearts. ErbB2 and ErbB4 expression did not change. The SFR to stretch evaluated in isolated papillary muscles was ≈130% of initial rapid phase in the shRNA-SCR group, while it was blunted in shRNA-EGFR–expressing muscles. Angiotensin II (Ang II)-dependent Na+/H+ exchanger 1 activation was indirectly evaluated by intracellular pH measurements in bicarbonate-free medium, demonstrating an increase in shRNA-SCR–injected myocardium, an effect not observed in the silenced group. Ang II- or EGF-triggered reactive oxygen species production was significantly reduced in shRNA-EGFR–injected hearts compared with that in the shRNA-SCR group. Chronic lentivirus treatment affected neither the myocardial basal redox state (thiobarbituric acid reactive substances) nor NADPH oxidase activity or expression. Finally, Ang II or EGF triggered a redox-sensitive pathway, leading to p90RSK activation in shRNA-SCR-injected myocardium, an effect that was absent in the shRNA-EGFR group.

***Conclusions*—**Our results provide evidence that specific EGFR activation after myocardial stretch is a key factor in promoting the redox-sensitive kinase activation pathway, leading to SFR development. **(*J Am Heart Assoc*. 2016;5:e004017 doi: 10.1161/JAHA.116.004017)**

Key Words: epidermal growth factor receptor • interference RNA • myocardial stretch

Increase in cardiac muscle length after a sudden stretch immediately leads to a larger contraction. This is classically attributed to enhanced myofilament responsiveness to calcium, and allows the heart to increase its output after a rise in preload or to maintain it despite a greater afterload. After this initial rise in contractility, myocardial performance slowly continues to increase, reaching a new steady state over the next 10 to 15 minutes. Genesis of this slow force response (SFR) to stretch, widely accepted to be the in vitro equivalent to the Anrep phenomenon, is still not fully understood. Cardiac hypertrophy and failure, two of the most important health problems in Western societies, are triggered by intracellular signals that occur following myocardial stretch. The stretch of cardiac muscle activates Angiotensin II (Ang II) receptor 1a (AT_1R), either by autocrine/paracrine release of endogenous Ang II or directly by mechanical forces

From the Centro de Investigaciones Cardiovasculares "Dr. Horacio E. Cingolani", Facultad de Ciencias Médicas, Universidad Nacional de La Plata, La Plata, Argentina (M.S.B., R.G.D., D.S.E., C.I.C., P.E.M., N.G.P.) and Laboratorio de Análisis de Imágenes, Facultad de Ciencias Veterinarias, Universidad Nacional de La Plata, Buenos Aires, Argentina (E.L.P.).

Accompanying Figures S1 and S2 are available at http://jaha.ahajournals.org/content/5/10/e004017/DC1/embed/inline-supplementary-material-1.pdf

*Dr Morgan and Dr Pérez contributed equally to this article.

Correspondence to: Néstor G. Pérez, PhD, Centro de Investigaciones Cardiovasculares "Dr. Horacio E. Cingolani", Facultad de Ciencias Médicas de La Plata, UNLP, 60 y 120 (1900) La Plata, Argentina. E-mail: gperez@med.unlp.edu.ar

Received June 16, 2016; accepted September 1, 2016.

(see[1] for review). Interestingly, the initial steps leading to the SFR involve similar cellular signals to those implicated in the development of these diseases.[2,3] SFR and cardiac hypertrophy are proposed to share the transactivation of the cardiac epidermal growth factor (EGF) receptor (EGFR) after AT_1R activation as a necessary step for their development (see[2] for review). The EGFR, or ErbB1, belongs to a protein tyrosine kinase family of four members, all expressed in normal adult rat hearts except for ErbB3.[4] Activation of these receptors is initiated after ligand binding and is followed by homodimerization or heterodimerization to produce transphosphorylation.[5] ErbB receptor family can be transactivated by a triple membrane–passing signal mechanism. G protein–coupled receptors, such as AT_1R, mediate activation of membrane-bound matrix metalloproteases, which cleave membrane-bound EGF-like ligands, provoking its shedding to the extracellular space to bind ErbB receptors.[5,6] Several models of cardiac hypertrophy suggest that EGFR transactivation by AT_1R is mediated by heparin-binding EGF (HB-EGF),[7,8] a ligand that is not exclusive of EGFR, also binding ErbB4.[9] Based on a report using a specific EGFR inhibitor, AG1478,[10] we showed that EGFR transactivation is required for the development of SFR following myocardial stretch of cat myocardium.[11] Although AG1478 preferentially inhibits EGFR with an IC_{50} of ≈3 nmol/L, at the reported doses (≈1 μmol/L), it could also inhibit ErbB4 activation.[12,13] Therefore, pharmacological inhibition of EGFR in vivo could provide systemic and unspecific inhibition. In the present study, we sought to specifically silence EGFR expression in the rat heart to avoid these inconveniences. A small hairpin RNA (shRNA) directed to the EGFR was incorporated into a lentiviral vector and injected into the left ventricular wall of adult Wistar rats. One month later, the myocardial EGFR-silencing effect on the proposed stretch-activated signaling pathway[2] was analyzed. Herein, we provide evidence to support that myocardial stretch activates the EGFR, a critical step for promoting the redox-sensitive kinase-mediated Na+/H+ exchanger 1 (NHE1) stimulation that leads to SFR development.

Materials and Methods

All procedures followed during this investigation conform to the Guide for the Care and Use of Laboratory Animals published by the US National Institutes of Health (NIH Publication No. 85-23, revised 1996) and to the guidelines by the Animal Welfare Committee of La Plata School of Medicine.

Molecular Biology

Plasmids for DNA transfection were prepared with a HiSpeed Plasmid Maxi Kit (cat. 12662; Qiagen) and alkaline lysis of *Escherichia coli* cells method.[14] Four different plasmids (three for the packaging proteins and one for the transgene expression) members of the lentivirus production system and mammalian expression plasmid for rat EGFR-GFP have previously been described (kind gift of Dr Jeffrey E. Segall, Albert Einstein College of Medicine, New York).[15]

Cell Culture

Lentiviral constructs and rat EGFR-GFP were expressed by transient transfection of HEK293T cells using the calcium phosphate method.[16] Cells were grown at 37°C in 5% CO_2 in DMEM, supplemented with 10% (v/v) fetal bovine serum and 1% (v/v) penicillin-streptomycin antibiotic.

Construction and Production of Lentiviral Vectors

A third-generation lentiviral plasmid containing DsRed reporter protein expressing an shRNA sequence against rat EGFR[17] was designed (p-shEGFR): 5′-cGCATAGGCATTGGTGAATT-3′ (positive strand), followed by: 5′-TTCAAGAGA-3′ (loop), 5′-AATTCACCAATGCCTATGCg-3′ (negative strand), and 5′-TTTTTT-3′ (terminator). This sequence was flanked by a *Bam*HI digestion site (5′) and a tandem of *Eco*RI-*Pac*I digestion sites (3′). An *Eco*RI site was used for screening purposes. Specificity of this sequence was confirmed with the Basic Local Alignment Search Tool (BLAST-NCBI): *E* value <0.001. A scrambled shEGFR nucleotide sequence, nonsilencing, was used as control (5′-ATGGCATTGCGATAAGTTG-3′, shSCR) and introduced in the expression vector (p-shSCR). Lentiviral particles were obtained, co-transfecting HEK293T cells with the four different plasmids. HEK293T cell media culture was collected at 24, 48, and 72 hours after transfection and immediately centrifuged for 10 minutes at 1000 *g*, virus containing supernatant was centrifuged for 2.5 hours at 50 000 *g*. Viral pellets were resuspended in PBS overnight at 4°C, aliquoted, and stored at −80°C. Lentivirus titer was determined measuring fluorescence of positive HEK293T cells transduced with serial dilutions of the viral stock in the presence of 8 μg/mL of polybrene (Sigma). Lentivirus encoding the nonsilencing sequence was used as control.

Intramyocardial Injection of the Lentivirus

Four-month-old male Wistar rats were anesthetized with sevoflurane (≈4% for induction and 2–3% for maintenance) used in a gas mixture with oxygen and delivered through ventilation by using a positive-pressure respirator (Model 680, Harvard). After reaching deep anesthesia, a left thoracotomy was performed via the fourth intercostal space and the lungs were retracted to expose the heart. Following this, the shRNA-EGFR or the shRNA-SCR lentivirus (≈2×10^7 transducing units

in 200 μL, multiplicity of infection ≈80) were injected at two sites in the free wall of the left ventricle, close to the cardiac apex, using a 30-gauge needle.[18,19] Immediately after surgery, rats were returned to their cages and carried to a recovery room and subsequently returned to the animal facility until sacrifice (1 month later). Rats had ad libitum access to food and water.

Echocardiography

Rats were monitored echocardiographically at the end of each protocol under light anesthesia with sevoflurane 4% by 2-dimensional M-mode echocardiography with a 7-MHz transducer. Measurements were performed according to the method proposed by the American Society of Echocardiography.

Isolation of Papillary Muscles, Force, and pH_i Determination

Papillary muscles from the left ventricle were used to assess the SFR to stretch, as previously described.[20] Briefly, the muscles were mounted in a perfusion chamber placed on the stage of an inverted microscope (Olympus) and superfused with a CO_2/HCO_3^-–buffered solution containing (mmol/L) NaCl 128.3, KCl 4.5, $CaCl_2$ 1.35, $NaHCO_3$ 20.23, $MgSO_4$ 1.05, and glucose 11.0, and equilibrated with 5% CO_2 to 95% O_2 (pH ≈7.40). Possible participation of catecholamines released by nerve endings was prevented by adrenergic receptor blockade (1.0 μmol/L prazosin plus 1.0 μmol/L atenolol). The muscles were paced at 0.2 Hz at a voltage 10% over threshold, maintained at 30°C, and isometric contractions were recorded. The cross-sectional area (calculated as 0.75 of the product of thickness and width) was used to normalize force records obtained with a silicon strain gauge (model AEM 801, Kronex Technologies Corp). The slack length of each muscle was determined after mounting, and the muscles were then progressively stretched to the length at which they developed maximal twitch force (Lmax). After a few minutes at Lmax, they were shortened to obtain 95% of the maximal twitch force (length that approximated 98% of Lmax and referred to as L98). Then, the muscles were shortened to 92% of Lmax (L92) and maintained at this length until the beginning of the stretching protocol to determine the SFR, which consisted in an abrupt stretch from L92 to L98.

The BCECF epifluorescence technique described elsewhere was used to measure intracellular pH (pH_i).[20] Briefly, after autofluorescence levels were recorded, the muscles were incubated for 1 hour in the BCECF-AM–containing solution. At the end of the loading period, washout of the extracellular space with dye-free solution was carried out for 30 to 60 minutes before any pH_i determination was performed. To limit photobleaching, a neutral-density filter (1% transmittance) was placed in the excitation light path. A manual shutter was used to alternatively select the excitation filters (440–495 nm). The experimental protocol used consisted in monitoring NHE1-mediated pH_i changes after applying a unique dose of Ang II (1 nmol/L) in muscles from shRNA-EGFR– and shRNA-SCR–injected rat hearts. The experiments were performed in the nominal absence of bicarbonate (HEPES buffer) to ensure that the only alkalizing operative pH_i regulatory mechanism was the NHE1. HEPES buffer solution was composed of (mmol/L) NaCl 146.2, KCl 4.5, $CaCl_2$ 1.35, $MgSO_4$ 1.05, glucose 11.0, and HEPES 10.0, titrated to pH 7.40 with NaOH and equilibrated with 100% O_2. At the end of each experiment, fluorescence emission was calibrated by the high KCl/nigericin method described elsewhere,[20] to transform experimental fluorescence ratios to pH_i values.

Measurement of $O_2^{\cdot}$ Production

Cardiac strips from the left ventricle (1×5 mm) were dissected and kept at 4°C until assayed. We used the lucigenin-enhanced chemiluminescence method to measure superoxide anion ($O_2^{\cdot}$) production, as previously described.[21] Briefly, cardiac slices were incubated in assay buffer in the absence or presence of Ang II (1 nmol/L) and EGF (0.1 μg/mL), during 30 minutes in a metabolic incubator under 95% O_2 to 5% CO_2 at 37°C before measuring $O_2^{\cdot}$. Chemiluminescence in arbitrary units was recorded with a luminometer (Chameleon; Hidex, Turku, Finland) during 30 seconds each at 4.5-minute intervals for 30 minutes. The lucigenin-containing assay buffer with tissue slices minus background and the responses to the drug assayed were reported. $O_2^{\cdot}$ production was normalized to milligrams dry weight tissue per minute.

Lipid Peroxidation

Lipid peroxidation was determined by measuring the rate of thiobarbituric acid reactive substances (TBARS) production, expressed as nmol/mg tissue. Heart homogenates were centrifuged at 2000*g* for 10 minutes. Supernatants (0.5 mL) were mixed with 1.5 mL trichloroacetic acid (30% w/v), 1 mL thiobarbituric acid (0.7% w/v), and 0.5 mL water, followed by boiling for 15 minutes. After cooling, absorbance was determined spectrophotometrically at 535 nm, using an ε value of 1.56×10^5 $(mol/L)^{-1}$ cm^{-1}.

NOX Activity

NADPH oxidase (NOX)–dependent superoxide production was measured in left ventricle homogenates from rats of both experimental groups, using a previously described lucigenin-enhanced chemiluminescence method.[22] Proteins were

diluted in modified HEPES buffer and distributed (100 μg/well) onto a 96-well microplate. NADPH (100 μmol/L) was added to wells just before reading. NOX activity measured by $O_2^{\cdot}$ production was expressed in cpm/mg of protein over 15 minutes.

Immunodetection

Tissue samples were prepared from freshly isolated heart left ventricle 1 month after lentiviral injection. The samples were rinsed with PBS buffer (mmol/L; NaCl 140, KCl 3, Na_2HPO_4 6.5, KH_2PO_4 1.5, and pH 7.4) and homogenized in RIPA lysis buffer (sc-24948), with a protease inhibitor cocktail and PMSF (sc-24948) and phosphatase inhibitor sodium orthovanadate (sc-24948). After a centrifugation of 13 000 *g* for 10 minutes at 4°C, protein concentration was determined in the supernatant fraction by the Bradford method. Samples were prepared by addition of SDS-PAGE sample buffer (20% [v/v] glycerol, 2% [v/v] 2-mercaptoethanol, 4% [w/v] SDS, 1% [w/v] bromophenol blue, 150 mmol/L Tris, pH 6.8) and 30 μg of protein. For the in vitro experiments, transiently transfected HEK293T cells were rinsed with PBS, and lysates of the whole tissue culture cells were prepared by addition of SDS-PAGE sample buffer. Prior to analysis, samples were sheared through a 26-gauge needle (Becton Dickinson). Samples were resolved by SDS-PAGE on 10% acrylamide gels. Proteins were transferred to polyvinylidene difluoride membranes by electrophoresis for 2 hours at 70 V at room temperature in buffer composed of 20% (v/v) methanol, Tris 25 mmol/L, and glycine 192 mmol/L. Polyvinylidene difluoride membranes were then blocked by incubation for 2 hours in T-TBS buffer (0.1% (v/v) Tween-20, NaCl 137 mmol/L, Tris 20 mmol/L, pH 7.5), containing 10% (w/v) nonfat dry milk, and then incubated overnight with the corresponding primary antibodies: polyclonal rabbit anti-EGFR, polyclonal rabbit anti-ErbB2, polyclonal rabbit anti-ErbB4, polyclonal rabbit anti P-p90RSK, polyclonal rabbit anti-P-ERK1/2, and monoclonal mouse GAPDH (Santa Cruz Biotechnology). Peroxidase-conjugated anti-rabbit, anti-mouse, and anti-goat (Santa Cruz Biotechnology) was used as secondary antibodies. Bands were visualized with enhanced chemiluminescence reagent (ECL, Millipore) and a Chemidoc Station (Bio-Rad) and quantified using Image J analysis software.

Confocal Imaging

Left ventricle samples were kept in buffered formalin during 24 hours and then serially cut into 10-μm-thick sections using a vibratome (Leica VT 1000S). Fluorescence was detected using a confocal microscope (Olympus FV1000). Solid-state laser at 559 nm was used for excitation of DsRed fluorophores. A ×4 objective was used for determining viral distribution in the tissue. For capturing the images, the intensity of the laser at 559 nm and of its photomultiplier were kept constant to qualitatively compare the samples.

Epifluorescence Microscopy

DsRed and GFP fluorescence images from HEK293T cells were obtained with an inverted Olympus 1X71 microscope equipped with a 100 W halogen lamp. Fluorescence emission was detected using 575 and 510 nm filters, respectively.

Statistics

Data are expressed as mean±SEM. Student *t* test or one-way ANOVA followed by Student-Newman-Keuls test, when appropriate, were used to compare data with n>4. Repeated-measures ANOVA was used to compare post-stretch force and post-Ang II pH_i data against time zero minute in each experimental group. Two-way ANOVA was used to compare post-stretch force and post-Ang II pH_i curves between groups. $P<0.05$ was considered statistically significant. Nonparametric statistic tests, Mann-Whitney or Kruskal-Wallis, were used to compare data samples with n≤4.

Results

Silencing capability of shEGFR cloned into the lentiviral transfer plasmid (p-shEGFR) was assessed in vitro in HEK293T. Cells were transiently transfected with increasing amounts of pEGFR-GFP and 48 hours later were lysed, electrophoresed, and immunoblotted with a specific antibody for EGFR. Figure 1A shows a strong protein expression of EGFR at its corresponding expected molecular weight (≈170 kDa). In contrast, cells transfected with an empty vector express little immunoreactive material. As expected, increasing expression of EGFR-GFP produces an increased green fluorescence visualized by epifluorescence (Figure 1B). Next, cells were co-transfected with a constant amount of the pEGFR-GFP (0.5 μg) and increasing concentrations of p-shEGFR. Since EGFR-GFP expression is driven by cytomegalovirus promoter as well as DsRed reporter protein contained in the p-shEGFR, plasmid transfection with lower amounts of p-shEGFR was compensated with p-shSCR. Consequently, reduced expression of EGFR would be the result of EGFR silencing and not less availability of DNA polymerase. Figure 1C shows an apparent EGFR expression reduction in cells expressing shEGFR. In accordance, silencing of GFP expression was evident by the significant reduction in green fluorescence without evident changes in red fluorescence (Figure 1D).

In order to explore the in vivo capability of the shRNA to silence the EGFR, silencing (shRNA-EGFR) and control

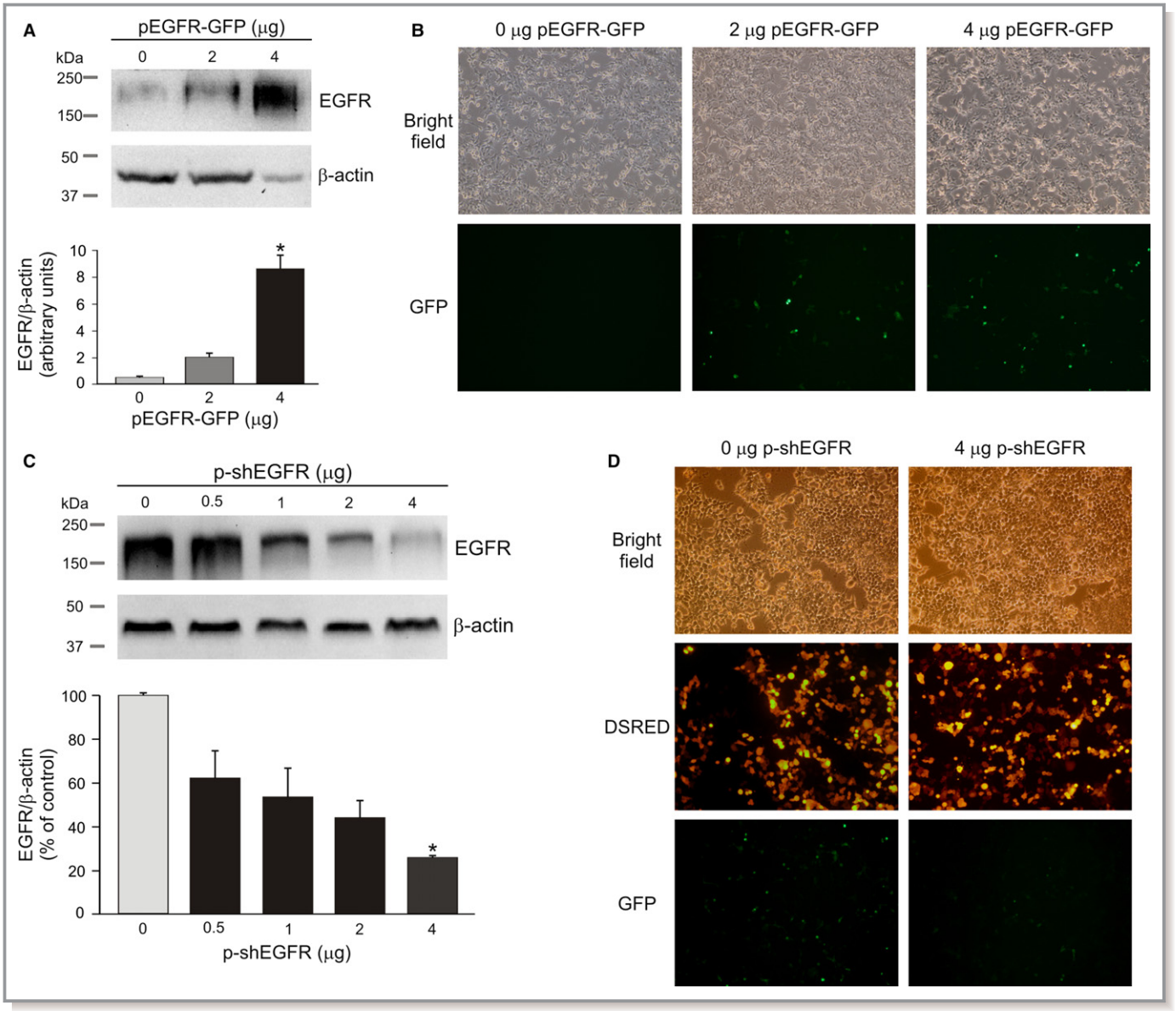

Figure 1. EGFR silencing in HEK293T cells. (A) Lysates of HEK293T cells transiently transfected with 0, 2, and 4 μg of EGFR-GFP plasmid were analyzed by electrophoresis and immunoblotted. Representative blots and averaged densitometry analysis results normalized to β-actin (each bar corresponds to n=3). (B) Fluorescent and bright-field images of the cell culture transfected with EGFR-GFP plasmid (×100). (C) Lysates of HEK293T cells were transiently co-transfected with 0.5 μg of EGFR-GFP plasmid and increasing concentrations of shRNA-EGFR coding plasmid (0, 0.5, 1, 2, and 4 μg, each bar corresponds to n=3). (D) Fluorescence microscope images of the cell cultures transfected with increasing amounts of p-shEGFR. (Kruskal-Wallis test [A], **P*<0.05 vs 0 μg pEGFR-GFP [C], **P*<0.05 vs 0 μg p-shEGFR.) EGFR indicates epidermal growth factor receptor; shRNA, small hairpin RNA.

(shRNA-SCR) lentivirus were injected into the rat myocardium at two different sites of the left ventricular free wall near the cardiac apex. Rats were euthanized 1 month later. Lentivirus spreading was determined by red fluorescence provided by DsRed protein expressed in heart left ventricle samples from shRNA-EGFR– and shRNA-SCR–injected animals, as well as from sham-operated animals (injected with PBS). A patchy red fluorescence distribution was observed in both groups of lentivirus-injected hearts, whereas no signal was detected in the sham-operated group (Figure S1). EGFR expression measured by immunoblots of left ventricle homogenates revealed ≈55% protein reduction in hearts injected with shRNA-EGFR compared with those injected with shRNA-SCR (Figure 2A). shEGFR expression did not affect myocardial expression of other closely related proteins such as the ErbB family members ErbB2 or ErbB4 (Figure 2B and 2C, respectively), strongly suggesting its specificity against EGFR.

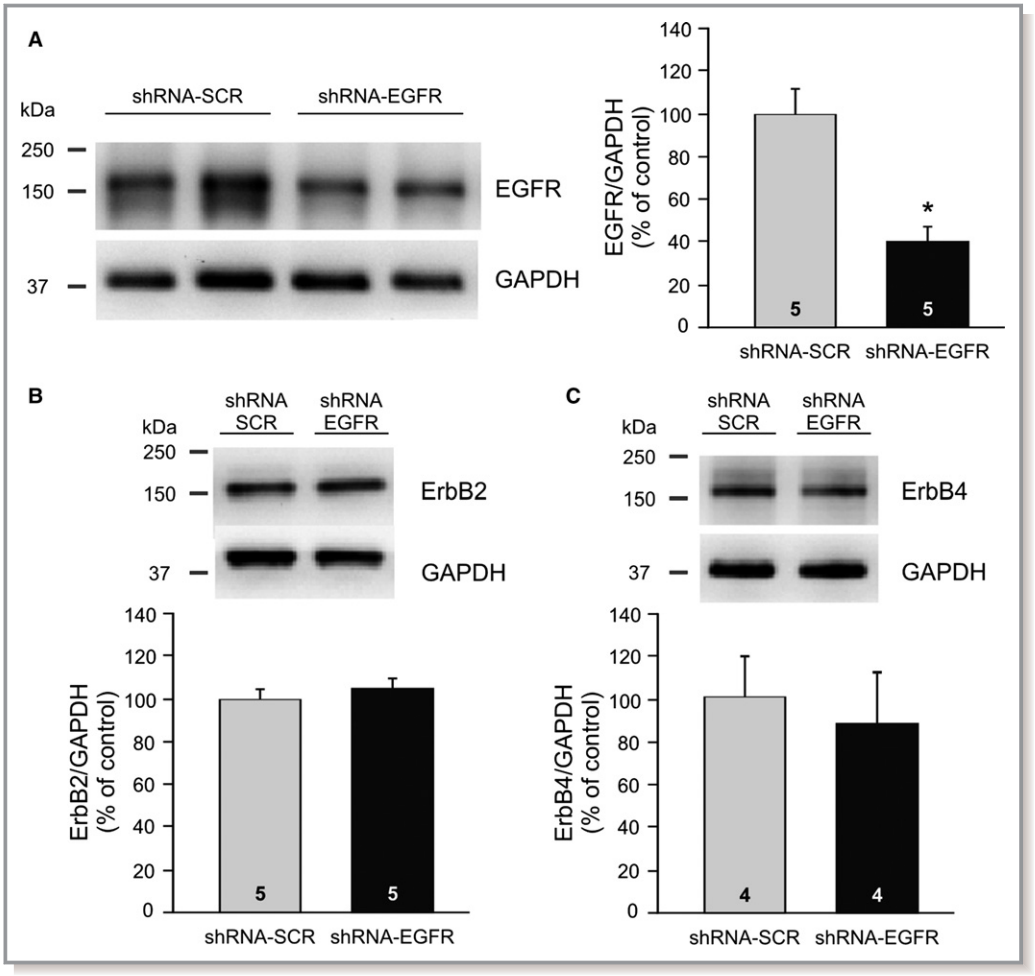

Figure 2. Left ventricular myocardium ErbB protein expression. Left ventricular tissue from shRNA-EGFR– or shRNA-SCR–injected hearts were homogenized and lysates analyzed by PAGE and immunoblotting. (A) Representative immunoblots showing EGFR expression of two different samples from each group (left), as well as the corresponding overall averaged results obtained from band densitometry analysis (right). (B and C) Myocardial expression of ErbB2 and ErbB4 members of the EGFR family. Representative immunoblots (top) and corresponding averaged results (bottom). ErbB expression was normalized to GAPDH expression. (*t* test [A and B], Mann-Whitney test [C], **P*<0.05 vs shRNA-SCR.) The number of independent experiments are included in the bars. EGFR indicates epidermal growth factor receptor; shRNA, small hairpin RNA.

We previously observed that SFR is inhibited by the protein tyrosin kinase inhibitor AG1478,[11] at a concentration of 1 μmol/L, which is also capable of inhibiting the ErbB4,[12,23] an alternative receptor for the HB-EGF and the endogenous ligand involved in the process. Therefore, we explored the functional consequences of chronic EGFR silencing in the heart. Echocardiographic and morphometric parameters were evaluated immediately before and after animal sacrifice, respectively. The Table shows that not significant differences between groups were found, suggesting that neither structure nor basal heart function was affected by chronic EGFR silencing.

The functional effect of EGFR silencing was analyzed on the SFR to sudden stretch. Stretching of isolated papillary muscles from the shRNA-SCR group promoted the characteristic biphasic mechanical response: an initial abrupt force increase (expression of the Frank-Starling mechanism) followed by the SFR (Figure 3A and 3C). However, when the same protocol was repeated in muscles from shRNA-EGFR–injected hearts, while the initial rapid phase was preserved, the SFR was completely canceled (Figure 3B and 3C), evidencing the key role played by the EGFR in this intrinsic mechanism, crucial to adapt cardiac output to changes in hemodynamic conditions.

Cardiac muscle alkalization after stretch in a bicarbonate-free medium is a consequence of AT_1R-mediated NHE1 activation.[24] To further characterize the functional effects of EGFR silencing in the myocardium, we evaluated pH_i changes in response to a low dose (1 nmol/L) of Ang II in both experimental groups in the nominal absence of bicarbonate.

Table. Morphometric and Echocardiographic Parameters From shRNA-SCR– and shRNA-EGFR–Injected Animals

	shRNA-SCR (n=8)	shRNA-EGFR (n=11)
Morphometric parameters		
BW, g	422.80±18.40	381.67±18.16
HW, g	1.01±0.04	0.90±0.04
LVW, g	0.80±0.04	0.72±0.03
TL, mm	42.26±0.44	41.23±0.31
HW/BW, $\times 10^{-3}$	2.40±0.06	2.36±0.04
LVW/BW, $\times 10^{-3}$	1.89±0.07	1.90±0.04
HW/TL, $\times 10^{-3}$ g/mm	23.91±0.87	21.85±0.72
LVW/TL, $\times 10^{-3}$ g/mm	18.83±0.87	17.58±0.61
Echocardiographic parameters		
LVDD, mm	6.32±0.15	6.23±0.13
LVSD, mm	2.46±0.08	2.42±0.09
FS, %	60.99±0.78	61.26±0.72
LVM, mg	706.46±30.61	680.99±26.96
LVM/BW, mg/g	1.67±0.06	1.80±0.04
LVM/TL, mg/mm	16.69±0.62	17.40±0.57
H/R	0.55±0.01	0.55±0.01

EGFR indicates epidermal growth factor receptor; FS, fractional shortening; H/R, relative wall thickness; LVDd indicates left ventricular end-diastolic dimension; LVSd, left ventricular end-systolic dimension; LVM, left ventricular mass; shRNA, small hairpin RNA. Body weight (BW), heart weight (HW), left ventricular weight (LVW), and tibia length (TL) were determined at necropsy. M-mode echocardiographic images were used to quantify cardiac function.

This Ang II dose was selected based on our previous work showing that it reproduces the signaling pathway triggered by the stretch, resulting in a similar force increment to the SFR.[25] Basal pH_i before addition of Ang II was similar in both groups of papillary muscles: 7.17±0.01 (n=7) in the shRNA-SCR group versus 7.18±0.01 (n=5) in the shRNA-EGFR group. A significant increase in pH_i was detected in muscles from shRNA-SCR–injected hearts (Figure 4A and 4B). This result would reflect NHE1 activation, since, in the absence of bicarbonate, it is the only operative alkalinizing mechanism. In contrast, when Ang II was added to shRNA-EGFR–injected muscles, pH_i moderately decreased instead of increased or even maintained basal values (Figure 4A and 4B). Although the available data do not explain the cause of this pH_i decrease in EGFR-silenced myocardium, at first glance we can conclude that these results, together with those presented in Figure 3, not only clearly indicate that EGFR activation is crucial for Ang II-triggered NHE1 stimulation, but also reinforce the notion of the key role played by EGFR transactivation in SFR development.

Increased NHE1 activity during stretch is dependent of reactive oxygen species (ROS) formation and activation of

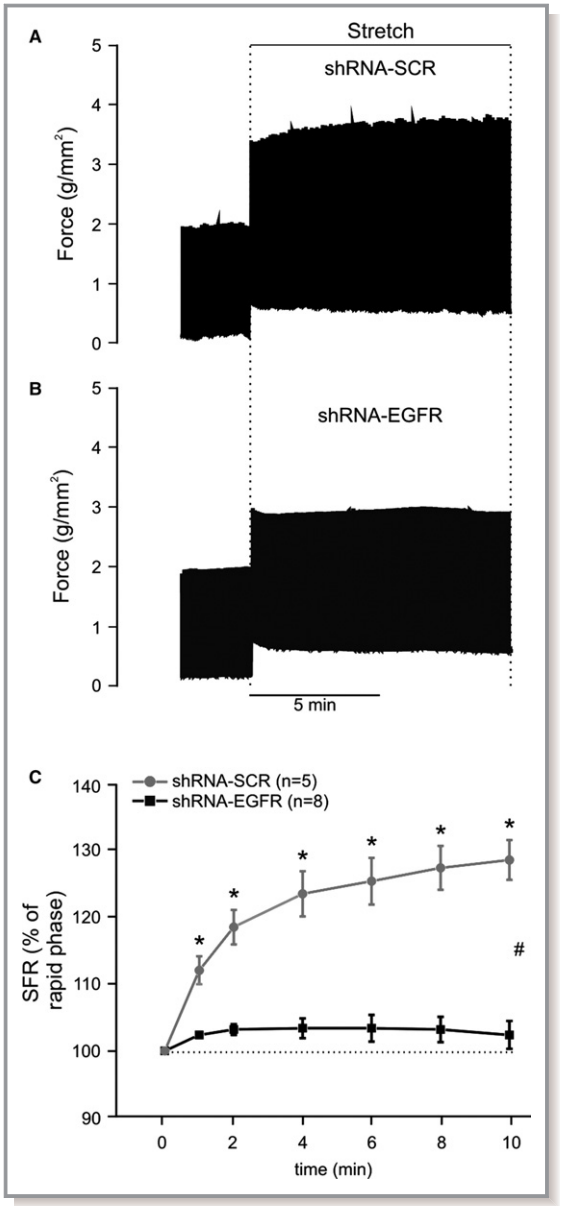

Figure 3. SFR and EGFR activation. (A) Original force record obtained in a papillary muscle from an shRNA-SCR–injected rat heart subjected to a sudden increase in length from 92% to 98% of Lmax. The biphasic force response to stretch, initial rapid followed by the SFR, can be observed. (B) Same as (A) but from a papillary muscle from a shRNA-EGFR–injected rat heart demonstrating that EGFR silencing blunt the SFR to stretch. (C) Average SFR data from both experimental groups expressed as percentage of the initial rapid phase (Frank-Starling mechanism). The SFR was calculated as the developed force (peak minus resting force) at indicated times compared with the developed force at the beginning of stretch (initial rapid phase=time zero minute), which was considered as 100%. (Repeated measures ANOVA, $^*P<0.05$ post-stretch force data vs time zero minute for each curve; two-way ANOVA, $^{\#}P<0.05$ post-stretch force curves comparison: shRNA-SCR vs shRNA-EGFR.) EGFR indicates epidermal growth factor receptor; SFR, slow force response; shRNA, small hairpin RNA.

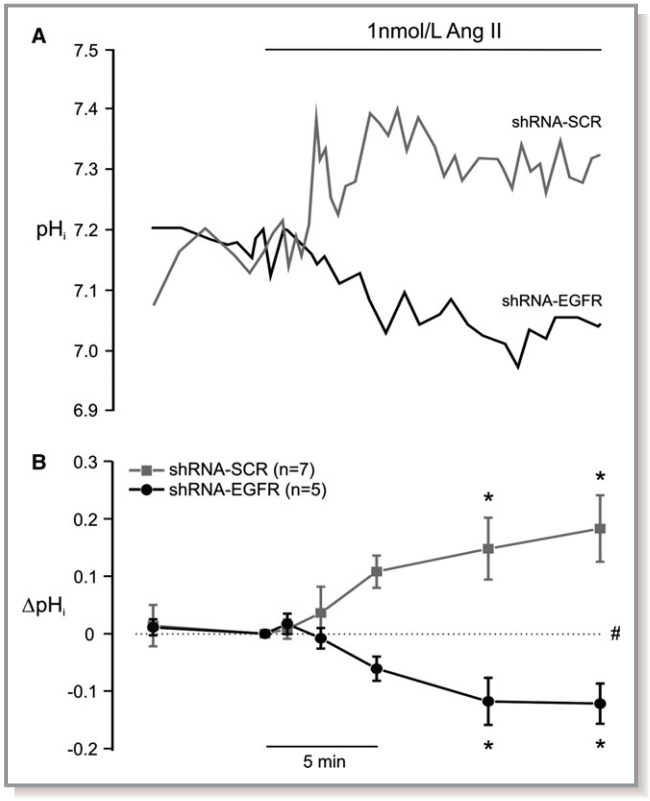

Figure 4. pH_i changes after Ang II stimulation. Isolated papillary muscles from shRNA-SCR– or shRNA-EGFR–injected hearts were loaded with pH-sensitive dye, BCECF, stabilized in bicarbonate-free solution and then stimulated with a low dose (1 nmol/L) of Ang II to explore the NHE1 activation. Ang II significantly increased pH_i in the shRNA-SCR group, an effect that was not observed in the EGFR-silenced group, as it can be appreciated in the original pH_i records shown in (A) as well as in the averaged results depicted in (B) (expressed as ΔpH_i=difference from pre-Ang II control). (Repeated measures ANOVA, $^*P<0.05$ post-Ang II pH_i data vs time zero minute (pre-Ang II control) for each curve; two-way ANOVA, $^{\#}P<0.05$ post-Ang II pH_i curves comparison: shRNA-SCR vs shRNA-EGFR). Ang II indicates angiotensin II; EGFR, epidermal growth factor receptor; NHE1, Na+/H+ exchanger 1; pHi, intracellular pH; shRNA, small hairpin RNA.

redox-sensitive kinases.[21] In the present study, cardiac left ventricle muscle strips were used to study myocardial $O_2^{\cdot}$ production in response to Ang II (1 nmol/L) or the specific EGFR agonist, EGF stimuli in both experimental groups. Figure 5A shows that Ang II significantly increased $O_2^{\cdot}$ production in cardiac samples of shRNA-SCR–injected hearts, whereas this effect was not observed in those in the EGFR-silenced group. Additionally, when an equipotent concentration of EGF (0.1 μg/mL) was used to directly stimulate the EGFR, a significant increase in $O_2^{\cdot}$ production was observed in the shRNA-SCR group, an effect that was completely abrogated in the cardiac strips of the shRNA-EGFR group (Figure 5A). Since EGFR activation increases ROS production, the chronic EGFR-silencing effect on basal redox homeostasis was analyzed. Lipid peroxidation estimated by quantifying TBARS in shRNA-SCR– or shRNA-EGFR–injected hearts was of the same magnitude (Figure 5B), indicating that oxidative stress was similar in both experimental groups. On the other hand, NOX2, one of the most important sources of O^{-}_2 in cardiac tissue that plays an important role in Ang II-induced cardiac hypertrophy,[26] can change its expression in response to different stimuli.[22] In the present study, total NOX activity (Figure 5C), as well as protein expression level of the NOX2 gp91 membrane subunit (Figure 5D), did not differ significantly between groups, indicating that it was not affected by chronic reduction of the EGFR expression.

We have previously demonstrated that ROS-sensitive kinases ERK1/2 and p90RSK are responsible for NHE1 activation during myocardial stretch.[21] Randomly selected cardiac left ventricle muscle strips from each heart was stimulated with Ang II (1 nmol/L) or EGF (0.1 μg/mL) for 15 minutes and frozen immediately after. Immunoblot analysis of homogenized samples revealed an increase in ERK1/2 and p90RSK phosphorylation in the shRNA-SCR group, an effect that was not observed in shRNA-EGFR samples (Figure 6A and 6B). Samples from shRNA-EGFR–injected hearts treated with Ang II produced a similar amount of ERK1/2 phosphorylation as the nonstimulated samples. Results from samples treated with EGF exposed a large mean and standard error, explained by the finding that one of the four samples analyzed presented an exceeded phosphorylation band compared with the rest of the samples. Duplicate analysis of this sample generated the same outcome. Overall analysis indicates that neither Ang II nor EGF stimulation of shRNA-EGFR–injected heart samples induced a significant increase in ERK1/2 or p90RSK phosphorylation. Total kinases expression measured on immunoblots revealed no modified expression of the silenced versus nonsilenced group (Figure S2).

Taken together, these data support the notion that EGFR activation after myocardial stretch is an important event of upstream myocardial ROS production leading to ERK1/2-p90RSK-NHE1 activation with consequent SFR development.

Discussion

Chronically sustained myocardial stretch in vivo derives in pathological cardiac hypertrophy. Acute myocardial stretch ex vivo originates the SFR. Both phenomena share a proposed initial EGFR transactivation by Ang II, mediated by HB-EGF.[2] This agonist has two natural receptors of the membrane protein tyrosine kinase family in the EGFR and ErbB4. In this study, we demonstrate that chronic and specific silencing of cardiac EGFR with interference RNA is enough to cancel the SFR, minimizing a potential role of the ErbB4 family member. Exogenous supply of Ang II to the shEGFR-expressing

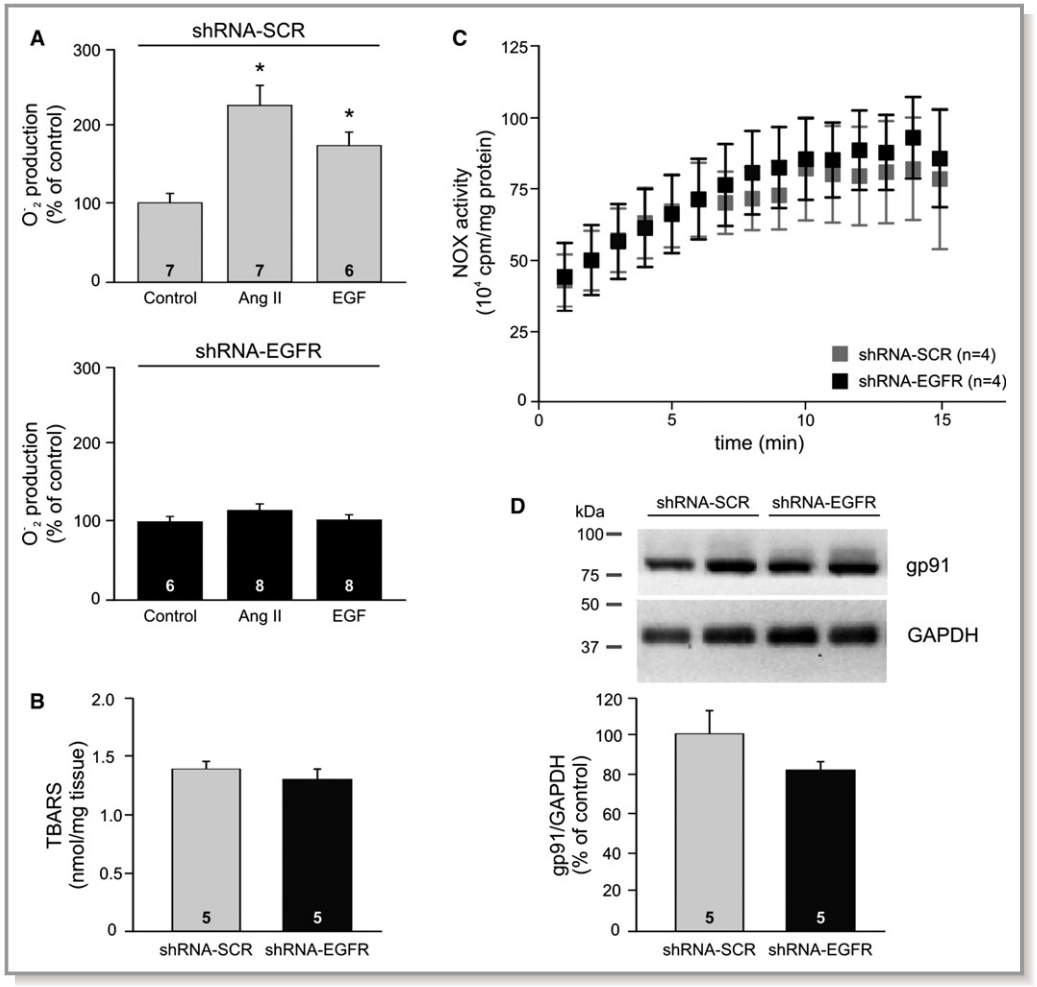

Figure 5. Myocardial superoxide anion production induced by Ang II or EGF. Cardiac strips from shSCR- or shEGFR-expressing hearts were stimulated with 1 nmol/L Ang II or 0.1 μg/mL EGF. While both significantly increased superoxide anion production in the scramble group, the effect was canceled in the EGFR-silenced group (A, results expressed as percentage of nonstimulated control). Importantly, left ventricle basal oxidative stress (B, estimated by lipid peroxidation through the TBARS method) as well as basal NOX activity (C, estimated by superoxide production) was not statistically different between groups. Furthermore, NOX gp91 membrane subunit protein expression level was not affected by the experimental procedure (D, representative immunoblots and corresponding averaged results from band densitometry analysis). (ANOVA, *P<0.05 vs control.) The number of independent experiments are included in the bars). Ang II indicates angiotensin II; EGF, epidermal growth factor; EGFR, EGF receptor; NOX, NADPH oxidase; shRNA, small hairpin RNA; TBARS, thiobarbituric acid reactive substances.

myocardium failed to stimulate active components of the SFR pathway, such as NHE1 transport, increased ROS production, and ERK1/2 or p90RSK protein kinases.

We previously observed that treatment with a protein tyrosine kinase inhibitor (PTKI), AG1478, cancelled the SFR together with the activation of several proposed components of the pathway. The AG1478 inhibitor was extensively described as a specific EGFR inhibitor with an IC_{50}=3 nmol/L[27] used in cardiac[7,11] and noncardiac[28] cells or tissues. AG1478 concentrations used in in vitro experiments are in a micromolar range, wich is far over EGFR IC50 and even over ErbB4 IC50 (allegedly, IC50=29.6 nmol/L). In fact, AG1478 in the micromolar range can also inhibit ErbB4 activation in tumoral cell lines[30] or cardiac cells.[12,23]

Normal ErbB4 activation by HB-EGF is essential for the adult heart. Cardiac ErbB2 and ErbB4 has shown a basal phosphorylation that is increased on perfusion with HB-EGF.[31] In contrast, in HB-EGF knockout mice, which present several hearts defects, a very low basal phosphorylation of cardiac ErbB2 and ErbB4 has been shown.[31] Also, in conditional cardiac ErbB4 knockout mice, dilated cardiomyopathy developed.[32] In addition, pharmacological use of AG1478, during cardiac studies of transactivation of EGFR, may have also affected ErbB4 with molecular and physiological consequences.

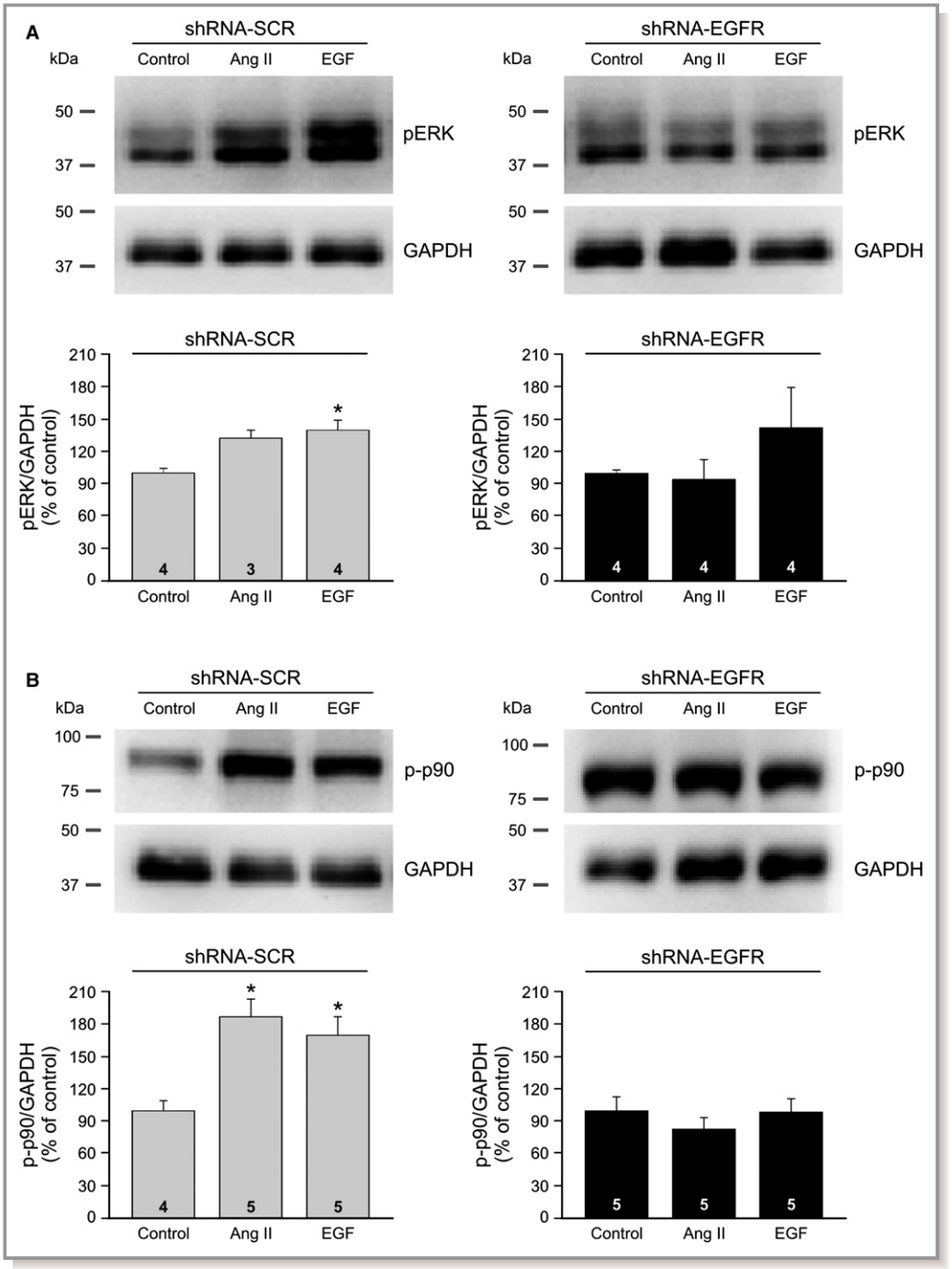

Figure 6. Cardiac ERK1/2 and p90RSK activation by Ang II or EGF stimulation. Cardiac tissue strips were incubated during 15 minutes either with Ang II (1 nmol/L) or EGF (0.1 μg/mL) and then homogenized, electrophoresed, and immunoblotted with specific antibodies to detect ERK1/2 (A) and p90RSK (B) phosphorylation. In the shRNA-SCR group, Ang II promoted a significant p90RSK phosphorylation/activation and a marginally significant increase in ERK1/2 (P=0.057), an effect that was not observed in the shRNA-EGFR group, as it can be appreciated in the representative blots (top of each panel) as well as in the corresponding averaged results (bottom of each panel). (Mann-Whitney test [A], t test [B], *P<0.05 vs nonstimulated control.) The number of independent experiments are included in the bars. Ang II indicates angiotensin II; EGF, epidermal growth factor; EGFR, EGF receptor; shRNA, small hairpin RNA.

We developed an shRNA to silence rat EGFR protein expression in vitro and specifically in vivo. By means of lentivirus, shEGFR was locally expressed in the heart to produce a ≈55% reduction of the protein expression without affecting ErbB2 or ErbB4 protein expression (Figure 2). EGFR protein expression reduction, although not complete, was

enough to prevent the SFR to stretch (Figure 3). DsRed fluorescence distribution observed in both groups of lentivirus-injected hearts (Figure S1) revealed a nonuniform lentivirus spreading from the injection site that left zones of EGFR expression unaffected, as shown previously.[33] Our rat models with a partial, specific, and local EGFR reduction in the heart, did not express cardiac hypertrophy or any other alteration of heart functional or morphometric parameters (Table). In contrast, knockout mice with complete EGFR inhibition in vascular smooth muscle cells and a partial reduction in cardiomyocytes had a phenotype with mean blood pressure reduction and cardiac hypertrophy.[34] Previously, we demonstrated that injection of a lentivirus in the heart produced negligible shRNA silencing in other organs.[18,19] Here, we did not measure EGFR expression away from the heart, and assume that EGFR expression was not changed in other tissues.

Increased ROS production is proposed as an early step along the pathway activated by Ang II during cardiac stretch or pathological cardiac hypertrophy.[2,35,36] Ang II (1 nmol/L) successively induces an increase in ROS production, activating ERK1/2 and p90RSK, which phosphorylate NHE1. This pathway would facilitate sodium entry to the cell and a secondary intracellular calcium increase. We showed that acute Ang II or EGF stimulation of left ventricle samples with partial reduction of EGFR was not able to induce ROS increase (Figure 5). Also, chronic cardiac expression of shEGFR did not induce any change in basal redox state or NOX activity. Our results suggest that EGFR expression is necessary to activate a ROS-mediated pathway activated by Ang II as described for the SFR. Previously, systemic administration of EGFR antisense oligonucleotides to rats prevented Ang II–induced ROS-sensitive ERK1/2 phosphorylation.[37] In contrast, EGFR knockout mice at the vascular smooth muscle cells, with a partial expression in cardiomyocytes, showed increased basal ROS production and NOX4 activity.[34] This apparent conflict likely reflects differences in the silencing time frame and/or tissue localization.

ROS-sensitive ERK kinases are influenced by ErbB4 signaling. It has been shown that HB-EGF administration to ErbB4-transfected HEK293 cells can induce ERK1/2 phosphorylation, and a similar phosphorylation amount was apparently obtained by neuregulin 1 (NRG1, a specific ErbB4 agonist) administration.[23] NRG1 in vitro administration to PC12 cells or to adult cardiomyocytes stimulates ERK1/2 phosphorylation, which is inhibited in a dose-dependent manner with AG1478. Our results show that the specific inhibition of cardiac EGFR is enough to avoid ERK1/2 activation by 1 nmol/L Ang II regardless of a potential contribution of ErbB4. These are similar results to those obtained by other authors[37] in rats treated with Ang II and EGFR antisense oligonucleotides as well as in a recently published paper on H9c2 cells.[38]

As previously mentioned, myocardial alkalization after stretch in a nominal bicarbonate-free condition is a manifestation of a stretch-triggered, AT_1R-mediated NHE1 activation.[24] In our study, AT_1R activation by a low dose of Ang II increased pH_i in papillary muscles from shRNA-SCR–injected hearts, whereas this effect was not observed in muscles from the shRNA-EGFR–injected group (Figure 4). We observed an unexpected decrease in pH_i after Ang II addition to the shRNA-EGFR group instead of remaining close to basal values. This finding would be explained if Ang II had affected the cardiac Slc26a6 anion exchanger, an acidifying pH_i regulatory mechanism that extrudes intracellular OH^- in exchange for extracellular Cl^-, and is negatively regulated by protein kinase C (PKC).[39] On one hand, PKC is responsible for the Ang II-triggered, NHE1-mediated increase in pH_i observed after myocardial stretch in bicarbonate-free conditions.[24] On the other hand, it has been shown that EGFR activation promotes PKC activation.[40] Therefore, Ang II may trigger EGFR-mediated PKC activation in shRNA-SCR, promoting PKC-mediated NHE1 activation as well as Slc26a6 anion exchanger inhibition. In EGFR-silenced myocardium, absence of PKC activation would avoid NHE1 activation but not Slc26a6 activity, which, by slowly extruding alkaline equivalents, would favor intracellular acidification. Beyond this unexpected finding, the observed result shows that at a low dose of Ang II, EGFR transactivation is crucial for myocardial alkalization likely due to NHE1 activation. Furthermore, we present conclusive evidence that specific inhibition of EGFR in the heart left ventricle allows cancellation of the SFR to stretch. Taken together, our current results strongly support the notion that myocardial stretch activates the EGFR, with this step being critical for promoting the redox-sensitive kinase-mediated NHE1 stimulation that leads to SFR development.

Conclusions

EGFR is widely expressed in normal tissues[41] where its activation is part of different physiological signaling pathways. However, activation of this receptor has also been associated with pathological conditions of the heart and vasculature, as well as with the development of diabetes and cancer.[42,43] Systemic administration of PTKIs to prevent activation of cardiac EGFR[38] can easily extend its action to other organs[44] or even to other proteins such as ErbB4.[45] Furthermore, it has been reported that clinical use of PTKIs during cancer treatment leads to cardiac toxicity.[43] Hence, local and specific EGFR inhibition with interference RNA may provide clear advantages as a potential therapeutic tool in cardiology clinical practice. In the present work, we show that specific inhibition of EGFR in the heart left ventricle allows cancellation of SFR to stretch. Since SFR and pathological cardiac hypertrophy are described to share a similar sequence of

molecule activation, local and specific EGFR inhibition could be considered as an alternative potential therapy for such cardiac disease.

Acknowledgments

The authors thank Oscar A. Pinilla for his invaluable technical help with the animal surgery and echocardiographic studies.

Sources of Funding

This work was supported in part by grant PICT 2012-2396 from Agencia Nacional de Promoción Científica y Tecnológica (ANPCyT) of Argentina to Dr Pérez, and PIP0433 from Consejo Nacional de Investigaciones Científicas y Técnicas (CONICET) of Argentina to Dr Morgan.

Disclosures

None.

References

1. Zablocki D, Sadoshima J. Solving the cardiac hypertrophy riddle: the angiotensin II-mechanical stress connection. *Circ Res*. 2013;113:1192–1195.
2. Cingolani HE, Perez NG, Cingolani OH, Ennis IL. The Anrep effect: 100 years later. *Am J Physiol*. 2013;304:H175–H182.
3. Ennis IL, Aiello EA, Cingolani HE, Perez NG. The autocrine/paracrine loop after myocardial stretch: mineralocorticoid receptor activation. *Curr Cardiol Rev*. 2013;9:230–240.
4. Zhao YY, Sawyer DR, Baliga RR, Opel DJ, Han X, Marchionni MA, Kelly RA. Neuregulins promote survival and growth of cardiac myocytes. Persistence of ErbB2 and ErbB4 expression in neonatal and adult ventricular myocytes. *J Biol Chem*. 1998;273:10261–10269.
5. Fuller SJ, Sivarajah K, Sugden PH. ErbB receptors, their ligands, and the consequences of their activation and inhibition in the myocardium. *J Mol Cell Cardiol*. 2008;44:831–854.
6. George AJ, Hannan RD, Thomas WG. Unravelling the molecular complexity of GPCR-mediated EGFR transactivation using functional genomics approaches. *FEBS J*. 2013;280:5258–5268.
7. Thomas WG, Brandenburger Y, Autelitano DJ, Pham T, Qian H, Hannan RD. Adenoviral-directed expression of the type 1A angiotensin receptor promotes cardiomyocyte hypertrophy via transactivation of the epidermal growth factor receptor. *Circ Res*. 2002;90:135–142.
8. Asakura M, Kitakaze M, Takashima S, Liao Y, Ishikura F, Yoshinaka T, Ohmoto H, Node K, Yoshino K, Ishiguro H, Asanuma H, Sanada S, Matsumura Y, Takeda H, Beppu S, Tada M, Hori M, Higashiyama S. Cardiac hypertrophy is inhibited by antagonism of ADAM12 processing of HB-EGF: metalloproteinase inhibitors as a new therapy. *Nat Med*. 2002;8:35–40.
9. Elenius K, Paul S, Allison G, Sun J, Klagsbrun M. Activation of HER4 by heparin-binding EGF-like growth factor stimulates chemotaxis but not proliferation. *EMBO J*. 1997;16:1268–1278.
10. Kuramochi Y, Cote GM, Guo X, Lebrasseur NK, Cui L, Liao R, Sawyer DB. Cardiac endothelial cells regulate reactive oxygen species-induced cardiomyocyte apoptosis through neuregulin-1beta/ErbB4 signaling. *J Biol Chem*. 2004;279:51141–51147.
11. Villa-Abrille MC, Caldiz CI, Ennis IL, Nolly MB, Casarini MJ, Chiappe de Cingolani GE, Cingolani HE, Perez NG. The Anrep effect requires transactivation of the epidermal growth factor receptor. *J Physiol*. 2010;588:1579–1590.
12. Icli B, Bharti A, Pentassuglia L, Peng X, Sawyer DB. ErbB4 localization to cardiac myocyte nuclei, and its role in myocyte DNA damage response. *Biochem Biophys Res Commun*. 2012;418:116–121.
13. Fukazawa R, Miller TA, Kuramochi Y, Frantz S, Kim YD, Marchionni MA, Kelly RA, Sawyer DB. Neuregulin-1 protects ventricular myocytes from anthracycline-induced apoptosis via ErbB4-dependent activation of PI3-kinase/AKT. *J Mol Cell Cardiol*. 2003;35:1473–1479.
14. Heilig JS, Elbing KL, Brent R. Large-scale preparation of plasmid DNA. *Curr Protoc Mol Biol*. 2001;chapter 1:unit 1.7.
15. Bailly M, Wyckoff J, Bouzahzah B, Hammerman R, Sylvestre V, Cammer M, Pestell R, Segall JE. Epidermal growth factor receptor distribution during chemotactic responses. *Mol Biol Cell*. 2000;11:3873–3883.
16. Jordan M, Wurm F. Transfection of adherent and suspended cells by calcium phosphate. *Methods*. 2004;33:136–143.
17. Feng M, Xiang JZ, Ming ZY, Fu Q, Ma R, Zhang QF, Dun YY, Yang L, Liu H. Activation of epidermal growth factor receptor mediates reperfusion arrhythmias in anaesthetized rats. *Cardiovasc Res*. 2012;93:60–68.
18. Nolly MB, Pinilla AO, Ennis IL, Cingolani HE, Morgan PE. Cardiac hypertrophy reduction in SHR by specific silencing of myocardial Na(+)/H(+) exchanger. *J Appl Physiol (1985)*. 2015;118:1154–1160.
19. Diaz RG, Perez NG, Morgan PE, Villa-Abrille MC, Caldiz CI, Nolly MB, Portiansky EL, Ennis IL, Cingolani HE. Myocardial mineralocorticoid receptor activation by stretching and its functional consequences. *Hypertension*. 2014;63:112–118.
20. Perez NG, de Hurtado MC, Cingolani HE. Reverse mode of the Na+-Ca2+ exchange after myocardial stretch: underlying mechanism of the slow force response. *Circ Res*. 2001;88:376–382.
21. Caldiz CI, Garciarena CD, Dulce RA, Novaretto LP, Yeves AM, Ennis IL, Cingolani HE, Chiappe de Cingolani G, Perez NG. Mitochondrial reactive oxygen species activate the slow force response to stretch in feline myocardium. *J Physiol*. 2007;584:895–905.
22. Bendall JK, Cave AC, Heymes C, Gall N, Shah AM. Pivotal role of a gp91(phox)-containing NADPH oxidase in angiotensin II-induced cardiac hypertrophy in mice. *Circulation*. 2002;105:293–296.
23. Chan HW, Jenkins A, Pipolo L, Hannan RD, Thomas WG, Smith NJ. Effect of dominant-negative epidermal growth factor receptors on cardiomyocyte hypertrophy. *J Recept Signal Transduct Res*. 2006;26:659–677.
24. Cingolani HE, Alvarez BV, Ennis IL, Camilion de Hurtado MC. Stretch-induced alkalinization of feline papillary muscle: an autocrine-paracrine system. *Circ Res*. 1998;83:775–780.
25. Perez NG, Villa-Abrille MC, Aiello EA, Dulce RA, Cingolani HE, Camilion de Hurtado MC. A low dose of angiotensin II increases inotropism through activation of reverse Na(+)/Ca(2+) exchange by endothelin release. *Cardiovasc Res*. 2003;60:589–597.
26. Byrne JA, Grieve DJ, Bendall JK, Li JM, Gove C, Lambeth JD, Cave AC, Shah AM. Contrasting roles of NADPH oxidase isoforms in pressure-overload versus angiotensin II-induced cardiac hypertrophy. *Circ Res*. 2003;93:802–805.
27. Levitzki A, Gazit A. Tyrosine kinase inhibition: an approach to drug development. *Science*. 1995;267:1782–1788.
28. Santra M, Chopp M, Santra S, Nallani A, Vyas S, Zhang ZG, Morris DC. Thymosin beta 4 up-regulates MIR-200a expression and induces differentiation and survival of rat brain progenitor cells. *J Neurochem*. 2016;136:118–132.
29. ReactionBiologyCorp. ErbB4/HER4. Available at: http://www.reactionbiology.com/webapps/site/KinasePDFs/ERBB4_HER4.pdf. Accessed December March 9, 2016.
30. Carrasco-Garcia E, Saceda M, Grasso S, Rocamora-Reverte L, Conde M, Gomez-Martinez A, Garcia-Morales P, Ferragut JA, Martinez-Lacaci I. Small tyrosine kinase inhibitors interrupt EGFR signaling by interacting with ErbB3 and ErbB4 in glioblastoma cell lines. *Exp Cell Res*. 2011;317:1476–1489.
31. Iwamoto R, Yamazaki S, Asakura M, Takashima S, Hasuwa H, Miyado K, Adachi S, Kitakaze M, Hashimoto K, Raab G, Nanba D, Higashiyama S, Hori M, Klagsbrun M, Mekada E. Heparin-binding EGF-like growth factor and ErbB signaling is essential for heart function. *Proc Natl Acad Sci USA*. 2003;100:3221–3226.
32. Garcia-Rivello H, Taranda J, Said M, Cabeza-Meckert P, Vila-Petroff M, Scaglione J, Ghio S, Chen J, Lai C, Laguens RP, Lloyd KC, Hertig CM. Dilated cardiomyopathy in Erb-B4-deficient ventricular muscle. *Am J Physiol*. 2005;289:H1153–H1160.
33. Perez NG, Nolly MB, Roldan MC, Villa-Abrille MC, Cingolani E, Portiansky EL, Alvarez BV, Ennis IL, Cingolani HE. Silencing of NHE-1 blunts the slow force response to myocardial stretch. *J Appl Physiol*. 2011;111:874–880.
34. Schreier B, Rabe S, Schneider B, Bretschneider M, Rupp S, Ruhs S, Neumann J, Rueckschloss U, Sibilia M, Gotthardt M, Grossmann C, Gekle M. Loss of epidermal growth factor receptor in vascular smooth muscle cells and cardiomyocytes causes arterial hypotension and cardiac hypertrophy. *Hypertension*. 2013;61:333–340.
35. Pimentel DR, Adachi T, Ido Y, Heibeck T, Jiang B, Lee Y, Melendez JA, Cohen RA, Colucci WS. Strain-stimulated hypertrophy in cardiac myocytes is

mediated by reactive oxygen species-dependent Ras S-glutathiolation. *J Mol Cell Cardiol*. 2006;41:613–622.

36. Sugden PH, Clerk A. Oxidative stress and growth-regulating intracellular signaling pathways in cardiac myocytes. *Antioxid Redox Signal*. 2006;8:2111–2124.
37. Kagiyama S, Eguchi S, Frank GD, Inagami T, Zhang YC, Phillips MI. Angiotensin II-induced cardiac hypertrophy and hypertension are attenuated by epidermal growth factor receptor antisense. *Circulation*. 2002;106:909–912.
38. Peng K, Tian X, Qian Y, Skibba M, Zou C, Liu Z, Wang J, Xu Z, Li X, Liang G. Novel EGFR inhibitors attenuate cardiac hypertrophy induced by angiotensin II. *J Cell Mol Med*. 2016;20:482–494.
39. Alvarez BV, Kieller DM, Quon AL, Markovich D, Casey JR. Slc26a6: a cardiac chloride-hydroxyl exchanger and predominant chloride-bicarbonate exchanger of the mouse heart. *J Physiol*. 2004;561:721–734.
40. Iwabu A, Smith K, Allen FD, Lauffenburger DA, Wells A. Epidermal growth factor induces fibroblast contractility and motility via a protein kinase C delta-dependent pathway. *J Biol Chem*. 2004;279:14551–14560.
41. Real FX, Rettig WJ, Chesa PG, Melamed MR, Old LJ, Mendelsohn J. Expression of epidermal growth factor receptor in human cultured cells and tissues: relationship to cell lineage and stage of differentiation. *Cancer Res*. 1986;46:4726–4731.
42. Forrester SJ, Kawai T, O'Brien S, Thomas W, Harris RC, Eguchi S. Epidermal growth factor receptor transactivation: mechanisms, pathophysiology, and potential therapies in the cardiovascular system. *Annu Rev Pharmacol Toxicol*. 2015;56:627–653.
43. Hervent AS, De Keulenaer GW. Molecular mechanisms of cardiotoxicity induced by ErbB receptor inhibitor cancer therapeutics. *Int J Mol Sci*. 2012;13:12268–12286.
44. Qian Y, Peng K, Qiu C, Skibba M, Huang Y, Xu Z, Zhang Y, Hu J, Liang D, Zou C, Wang Y, Liang G. Novel epidermal growth factor receptor inhibitor attenuates angiotensin II-induced kidney fibrosis. *J Pharmacol Exp Ther*. 2016;356:32–42.
45. Li XM, Su F, Ji MH, Zhang GF, Qiu LL, Jia M, Gao J, Xie Z, Yang JJ. Disruption of hippocampal neuregulin 1-ErbB4 signaling contributes to the hippocampus-dependent cognitive impairment induced by isoflurane in aged mice. *Anesthesiology*. 2014;121:79–88.

SUPPLEMENTAL MATERIAL

Figure S1

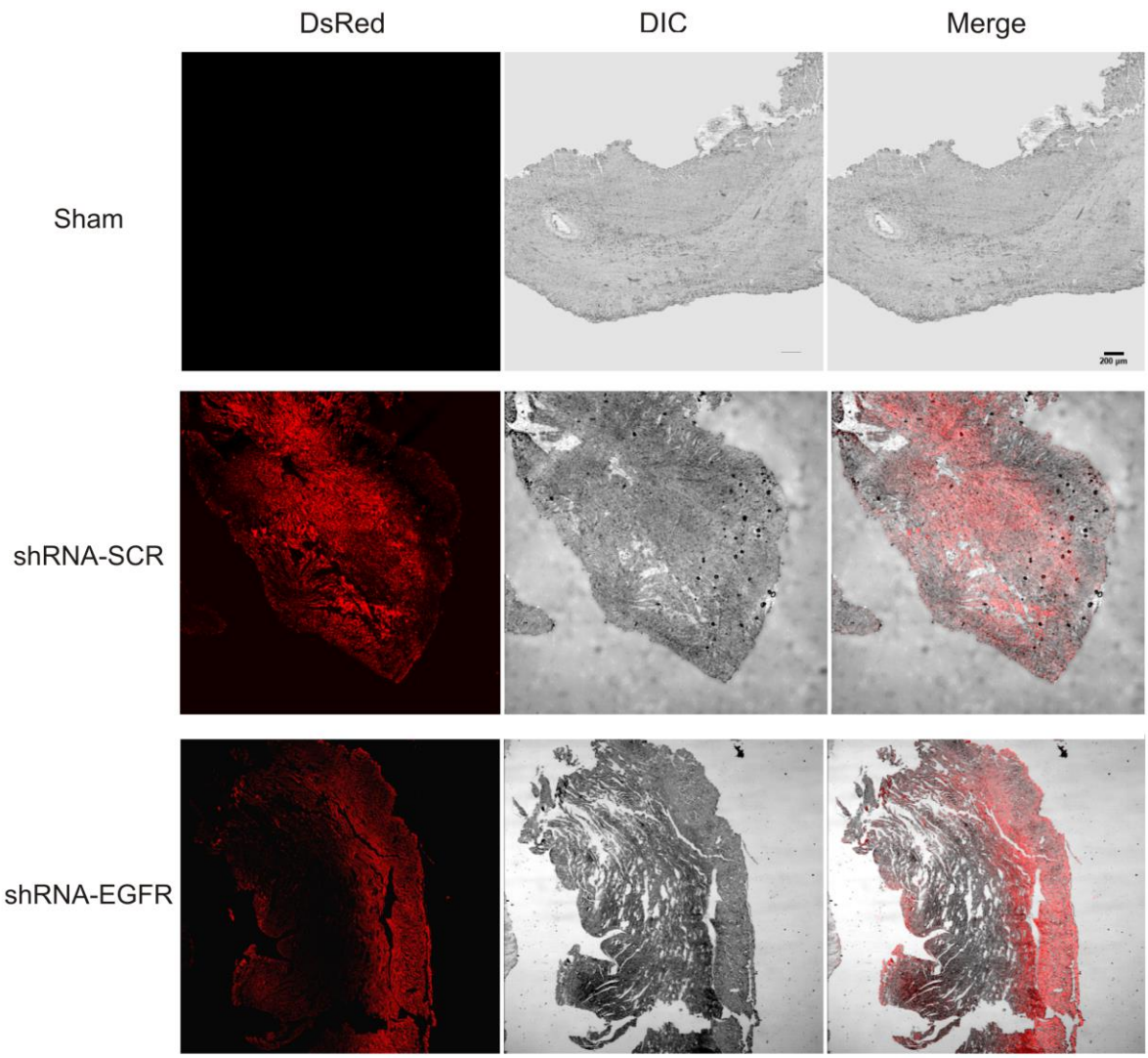

Figure S1. **Myocardial distribution of the lentivirus**. Representative confocal images (4X) of myocardial slices from hearts injected with shRNA-EGFR or shRNA-SCR lentiviral vectors, as well as from a sham-operated rat. Characteristic patchy distribution of red fluorescence due to DsRed protein can be observed. The second column presents confocal captures from the same slices using different interference contrast (DIC). The third column represents merging images obtained from the previous ones (bar = 200 μm).

Figure S2

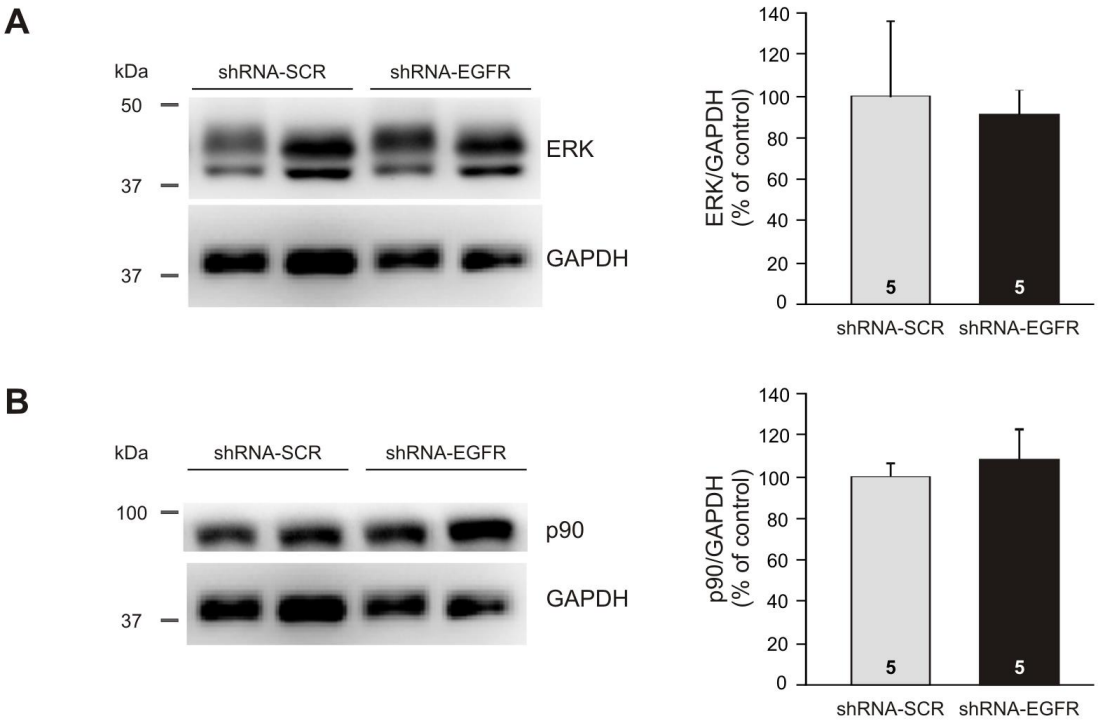

Figure S2. **Left ventricular ERK1/2 and p90RSK protein expression**. Left ventricular stripes expressing shRNA-EGFR or shRNA-SCR were homogenized and lysates analyzed by PAGE and immunobloting. Expression of both kinases was unaffected by the experimental procedure as it can be appreciated in the representative immunoblots for ERK1/2 (A) and p90RSK (B), as well as in the corresponding averaged results (t-test). Expression was normalized to GAPDH protein expression.